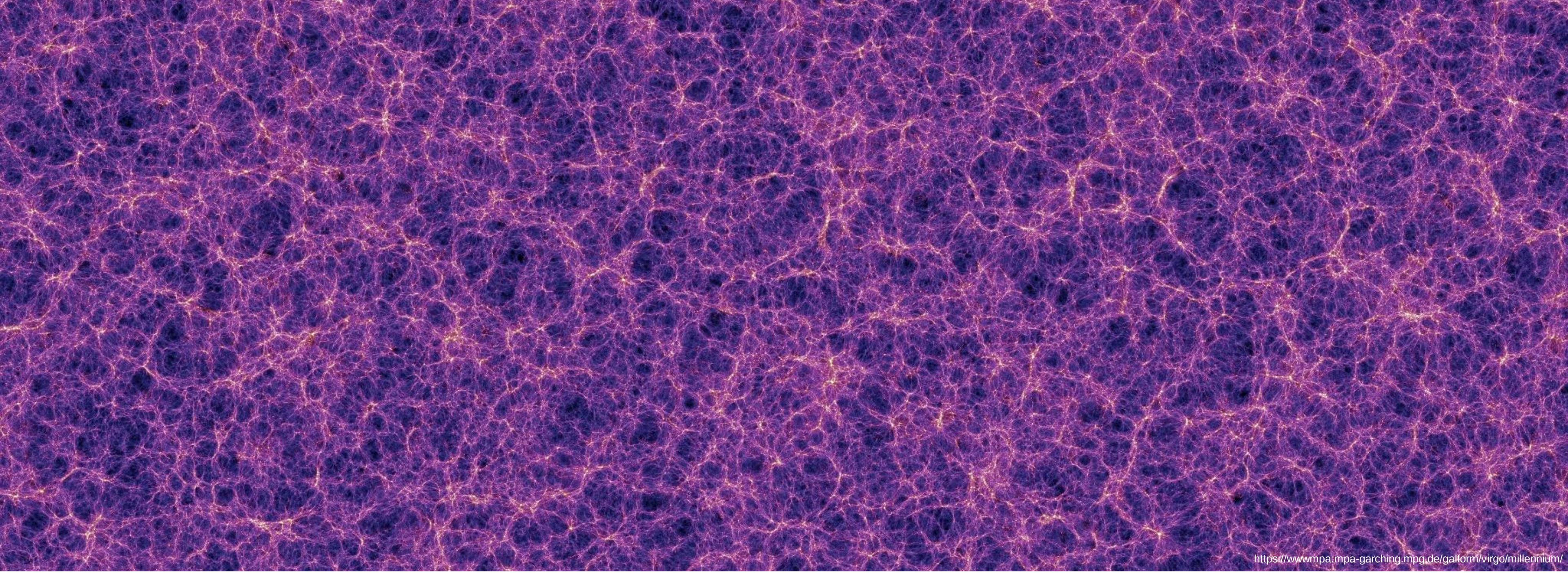

Calculation of Large Scale Structure Power Spectra in a Spherical-Fourier Bessel (SFB) Basis

Presented by Brandon Khek, Rice University
Mentors: Olivier Doré and Henry Gebhardt, JPL, Caltech
October 23, 2021

RICE

Matter power spectra are a statistical tool used to constrain cosmological expansion

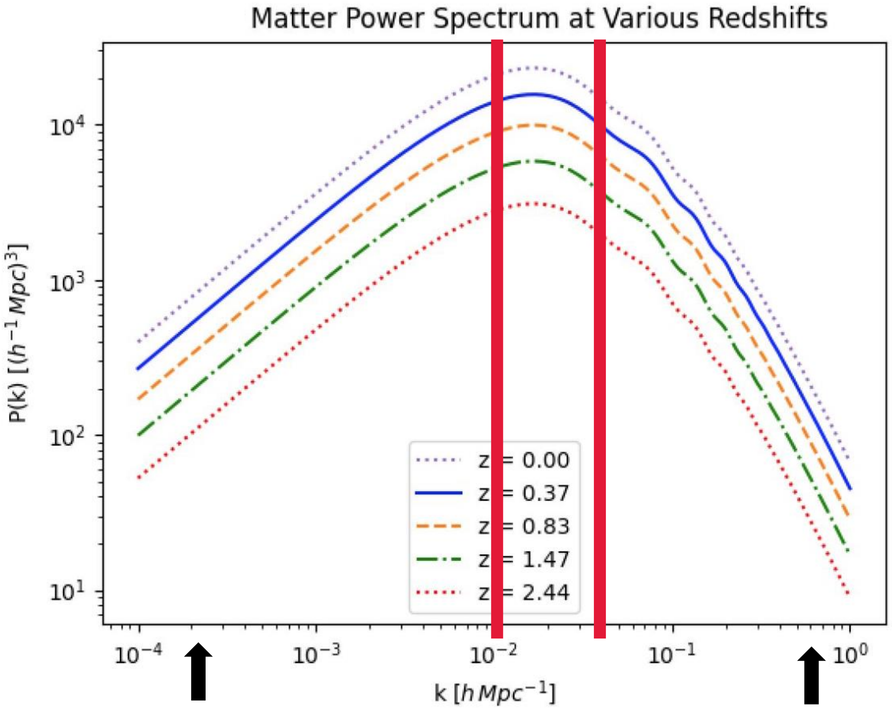

Larger scales

Smaller scales

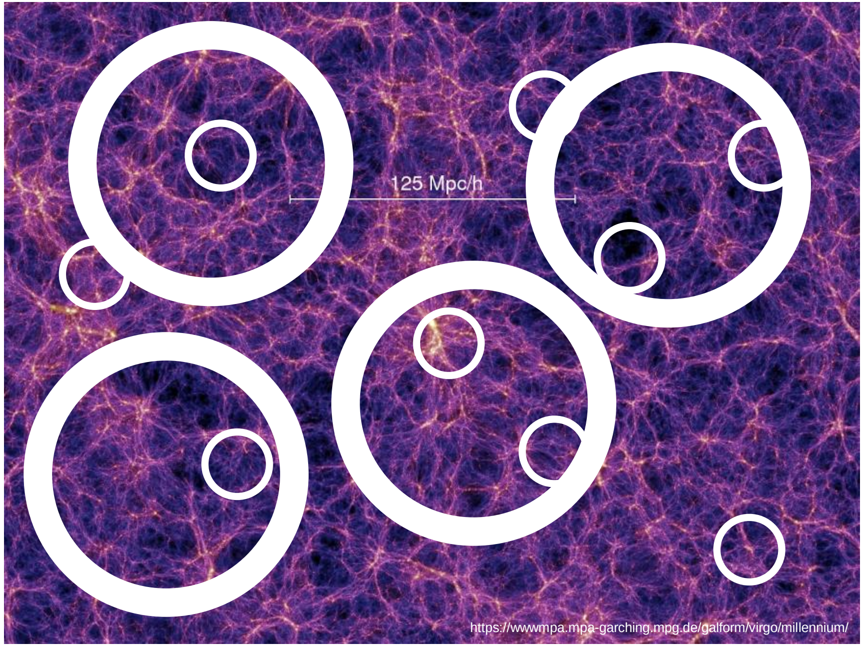

Physical effects appear in the power spectrum and help us understand structure in the universe

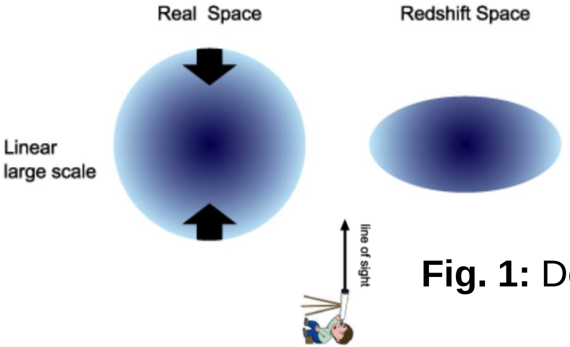

Fig. 1: Depiction of RSD[1]

Physical effects considered

- Redshift space distortions (RSD)
- Baryon acoustic oscillations (BAO)
- Non-Gaussianity (NG)

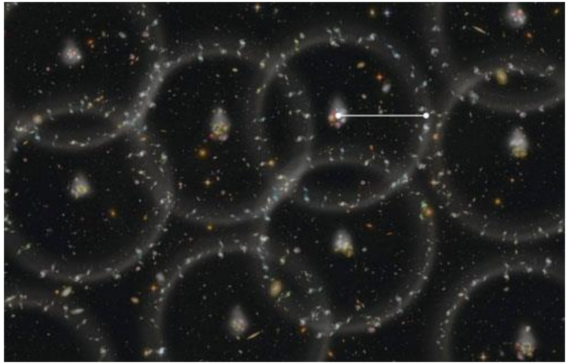

Fig. 2: Cartoon of BAO[2]

Fig. 3: NG representation

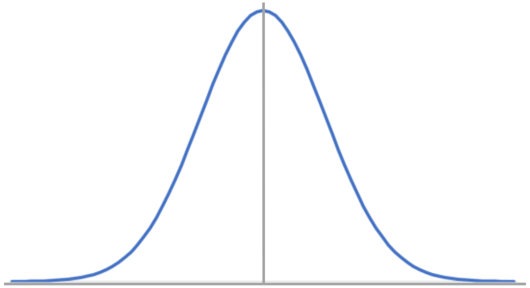

[1] S. Saito, Galaxy Clustering in Redshift Space, 2016, [2] BOSS Collaboration

Next-generation galaxy surveys will give us a 3-D map of the universe

E.g. SPHEREx, Nancy Grace Roman Space Telescope

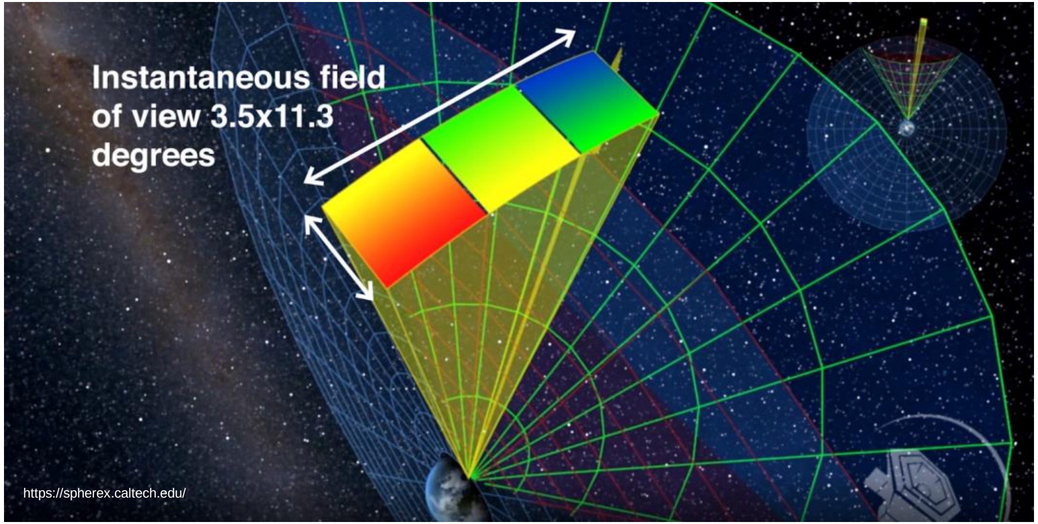

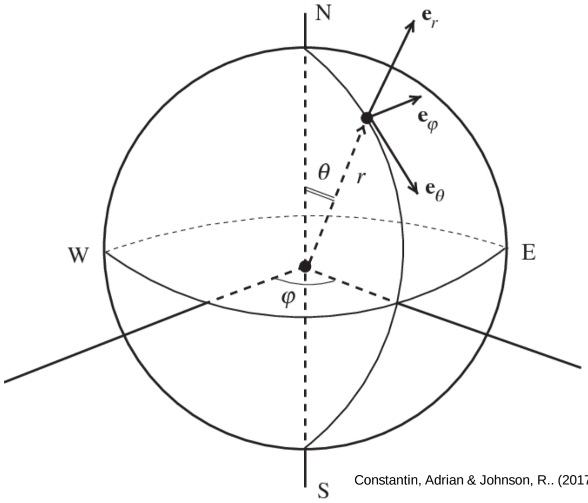

Constantin, Adrian & Johnson, R.. (2017)

We developed code to calculate the SFB power spectrum to account for wide-angle effects in upcoming surveys

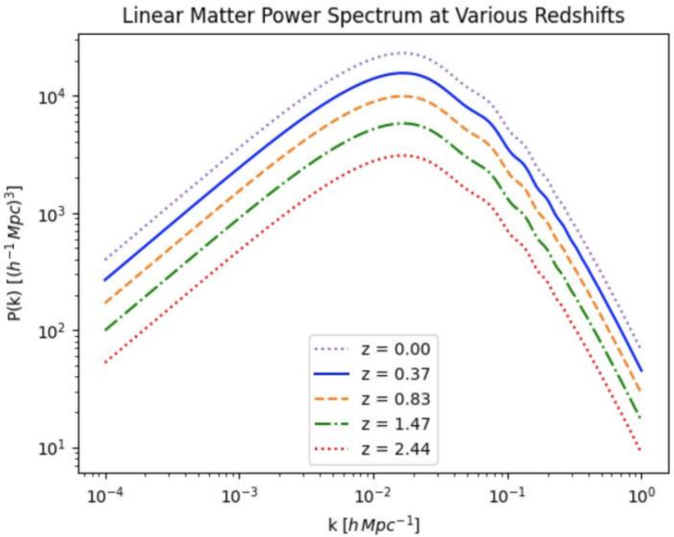

Project

$$P(k) \to C_\ell(k, k')$$

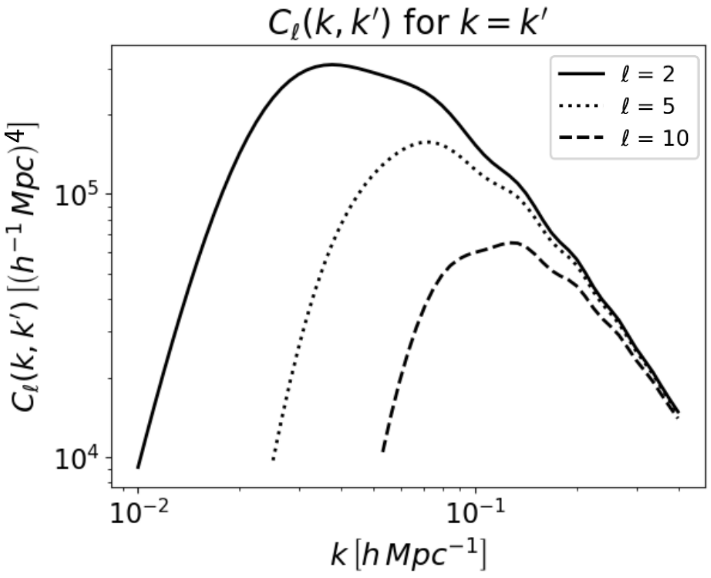

Clustering amplitude is amplified by RSD and BAO

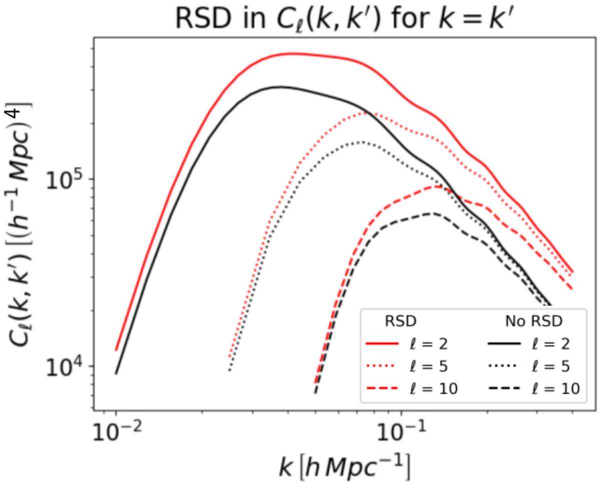

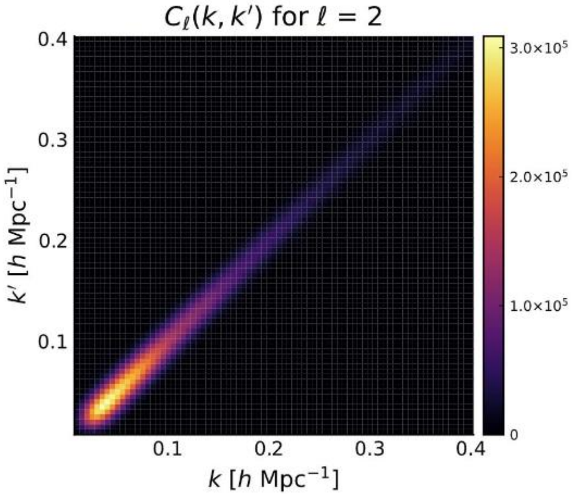

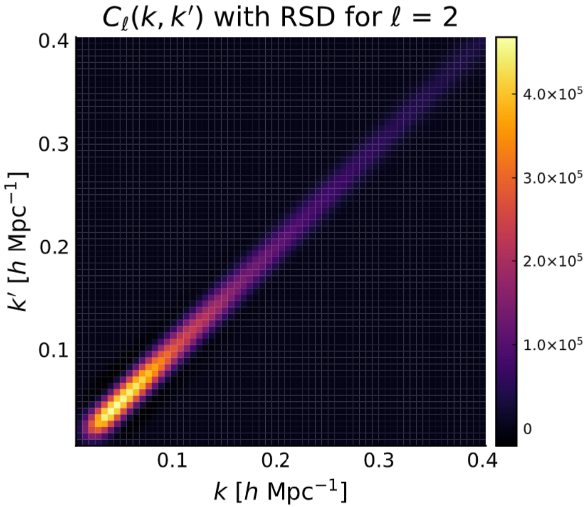

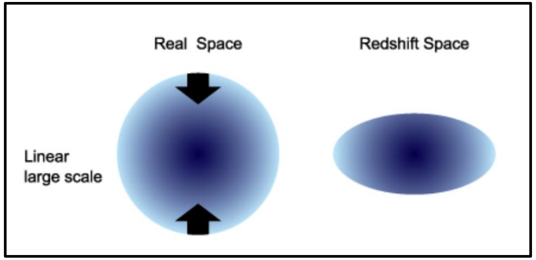

Depiction of RSD

Non-Gaussianity is evidenced by more clustering on larger scales

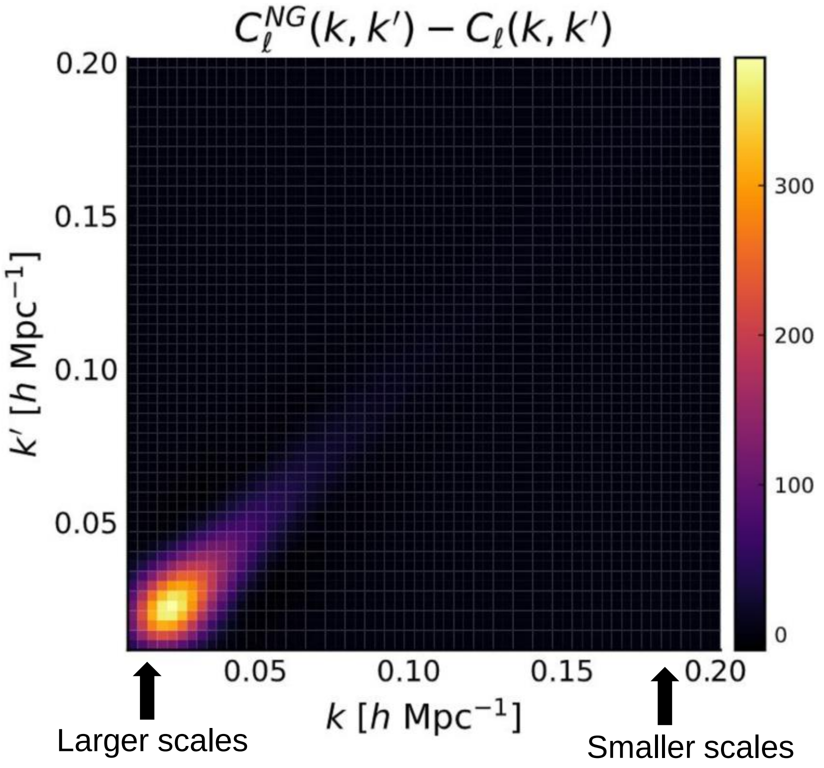

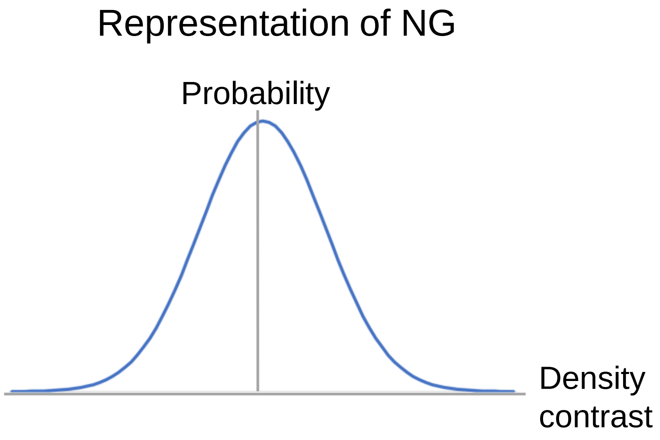

Error arises from precision in our numerical integration

ℓ	k Range	Average % Error	Time (s)
2	0.01 to 0.3	$1.7 * 10^{-11}$	1.71
10	0.05 to 0.4	$1.1 * 10^{-4}$	1.27
50	0.15 to 0.5	$1.2 * 10^{-2}$	5.37

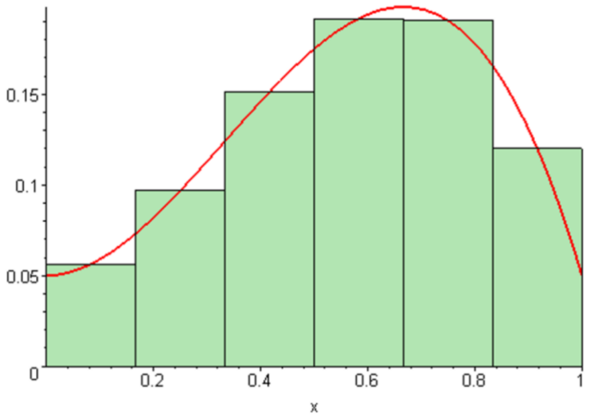

Compare to obtain error

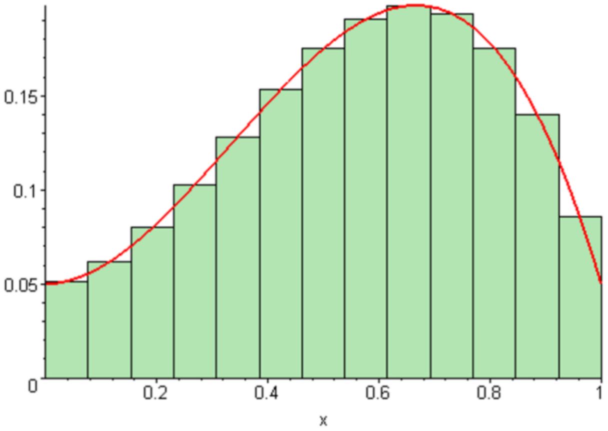

https://en.wikipedia.org/wiki/Riemann_sum

Analysis of modified gravity, performance improvements, and studying off-diagonal terms is underway

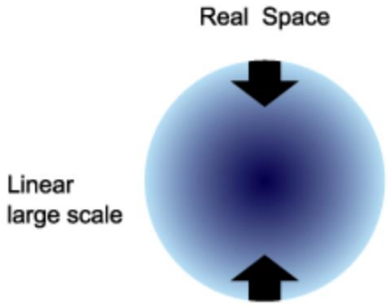

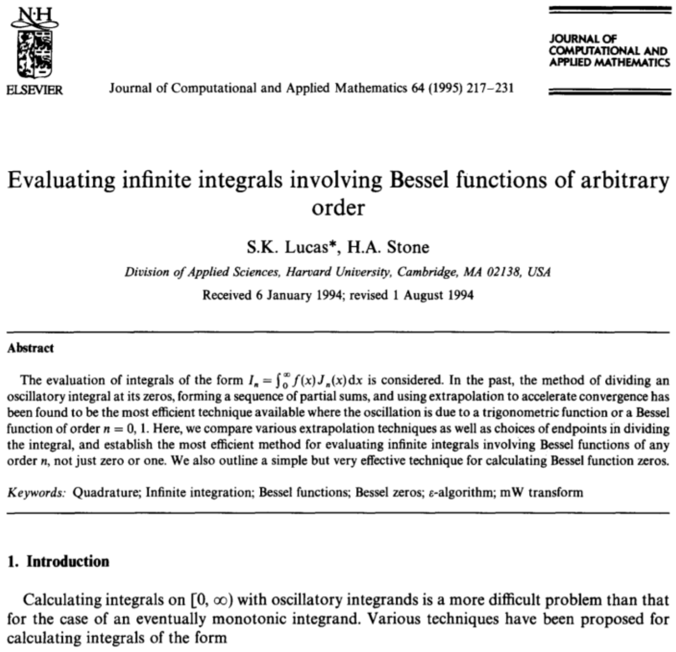

N·H
ELSEVIER

Journal of Computational and Applied Mathematics 64 (1995) 217–231

JOURNAL OF COMPUTATIONAL AND APPLIED MATHEMATICS

Evaluating infinite integrals involving Bessel functions of arbitrary order

S.K. Lucas*, H.A. Stone

Division of Applied Sciences, Harvard University, Cambridge, MA 02138, USA

Received 6 January 1994; revised 1 August 1994

Abstract

The evaluation of integrals of the form $I_n = \int_0^\infty f(x) J_n(x)\,dx$ is considered. In the past, the method of dividing an oscillatory integral at its zeros, forming a sequence of partial sums, and using extrapolation to accelerate convergence has been found to be the most efficient technique available where the oscillation is due to a trigonometric function or a Bessel function of order $n = 0, 1$. Here, we compare various extrapolation techniques as well as choices of endpoints in dividing the integral, and establish the most efficient method for evaluating infinite integrals involving Bessel functions of any order n, not just zero or one. We also outline a simple but very effective technique for calculating Bessel function zeros.

Keywords: Quadrature; Infinite integration; Bessel functions; Bessel zeros; ε-algorithm; mW transform

1. Introduction

Calculating integrals on $[0, \infty)$ with oscillatory integrands is a more difficult problem than that for the case of an eventually monotonic integrand. Various techniques have been proposed for calculating integrals of the form

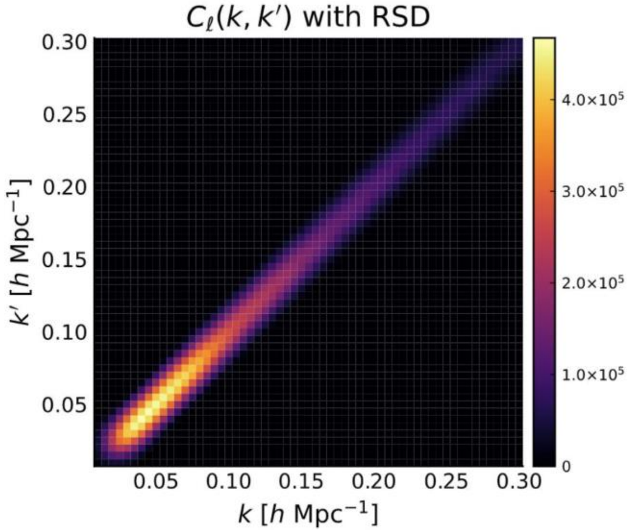

Acknowledgements

Henry Gebhardt and Olivier Doré

Jet Propulsion Laboratory

Caltech Student-Faculty Programs

Jet Propulsion Laboratory
California Institute of Technology

CALTECH
Student-Faculty Programs

Main Takeaways

The matter power spectrum helps us understand the expansion of space and nature of the universe

We developed code to calculate the matter power spectrum in a spherical Fourier Bessel basis

This code provides a crucial step in the analysis of upcoming galaxy surveys like SPHEREx or NGRST

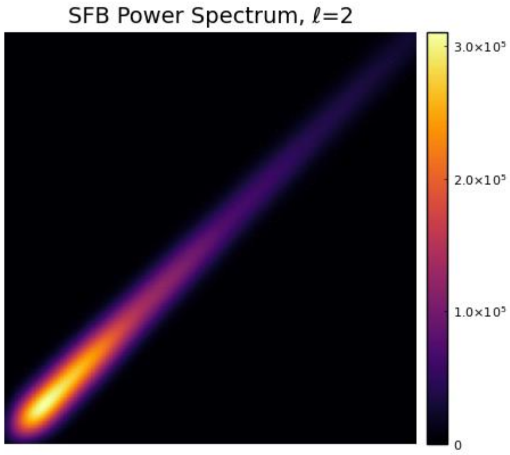

Spherical harmonics are the Fourier basis on the surface of sphere

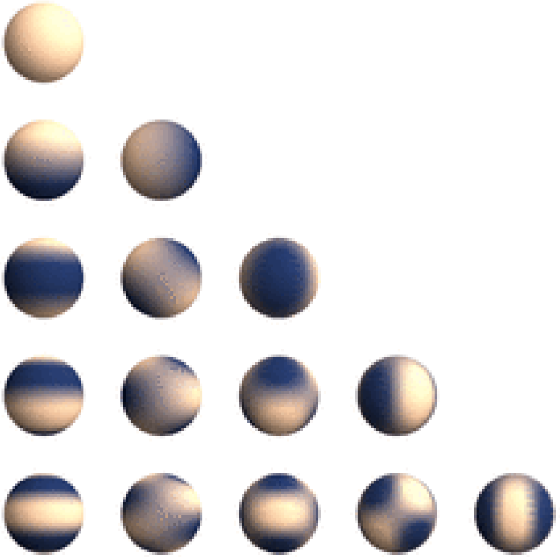

Real (Laplace) spherical harmonics $Y_{\ell m}$ for $\ell = 0, \ldots, 4$ (top to bottom) and $m = 0, \ldots, \ell$ (left to right). Zonal, sectoral, and tesseral harmonics are depicted along the left-most column, the main diagonal, and elsewhere, respectively. (The negative order harmonics $Y_{\ell(-m)}$ would be shown rotated about the *z* axis by $90^\circ/m$ with respect to the positive order ones.)

https://en.wikipedia.org/wiki/Spherical_harmonics

Formula for the continuous SFB power spectrum

$$C_\ell(k,k') = \int \mathrm{d}q\, \mathcal{W}_\ell(k,q)\, \mathcal{W}^*_\ell(k',q)\, P(q) \tag{1}$$

$$\mathcal{W}_\ell(k,q) = \frac{2qk}{\pi} \int \mathrm{d}r\, r^2\, \phi(r)\, D(r)\, b(r,q)\, j_\ell(kr) \times e^{-\frac{1}{2}\sigma_u^2 q^2} \sum_{\Delta\ell} \left(\delta^K_{\Delta\ell,0} - \beta f^\ell_{\Delta\ell}\right) j_{\ell+\Delta\ell}(qr) \tag{2}$$

https://arxiv.org/pdf/2102.10079.pdf

Formula for the discrete SFB power spectrum

$$\langle \delta_{n\ell m}\, \delta_{n'\ell m} \rangle = \int \mathcal{W}_{n\ell}(q) \mathcal{W}_{n'\ell}(q) P(q)\, dq \qquad (1)$$

$$\mathcal{W}_{n\ell}(q) = \sqrt{\frac{2q^2}{\pi}} \int_{r_{\min}}^{r_{\max}} g_{n\ell}(r)\, \Upsilon_\ell(r,q)\, r^2 dr \qquad (2)$$

$$\Upsilon_\ell(r,q) = \phi(r) D(r) b(r,q) \sum_{\Delta\ell} (\delta^K_{\Delta\ell,0} - \beta f^\ell_{\Delta\ell}) j_{\ell+\Delta\ell}(qr) \qquad (3)$$

Why NG results in larger structures at large scales

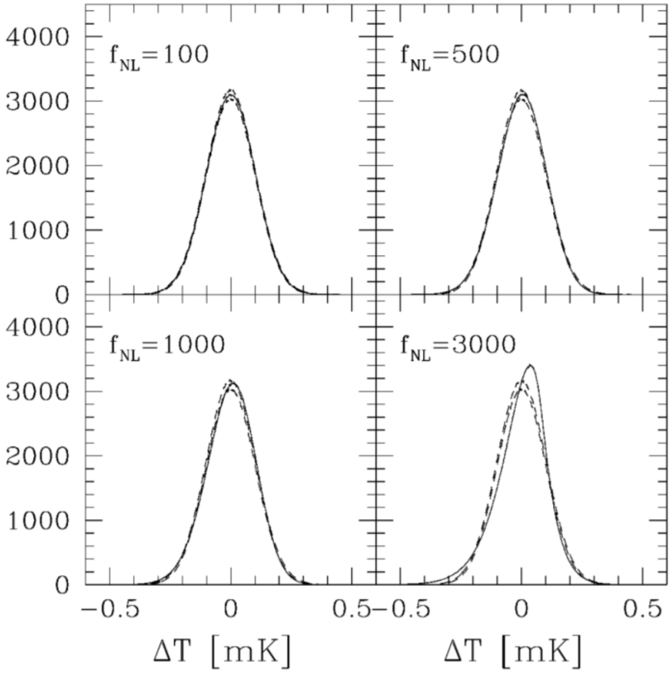

https://wwwmpa.mpa-garching.mpg.de/~komatsu/presentation/fnl.pdf

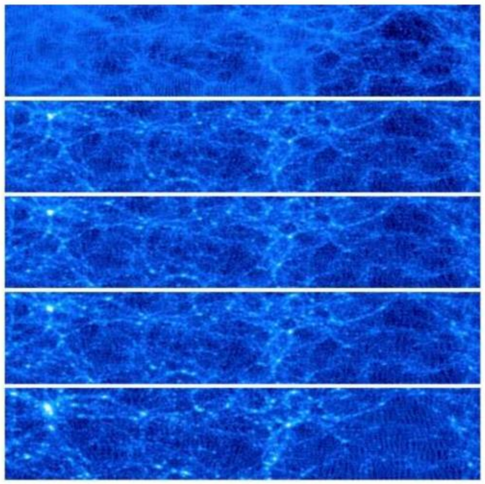

FIG. 1: Slice through simulation outputs at $z = 0$ generated with the same Fourier phases but with $f_{\rm NL} = -5000$, -500, 0, $+500$, $+5000$ respectively from top to bottom. Each slice is 375 h^{-1} Mpc wide, and 80 h^{-1} Mpc high and deep. We can easily match by eye much of the large scale structure; for example, an overdense region sits on the left, while an underdense region (void) falls on the right, in all panels. Note that for positive $f_{\rm NL}$, overdense regions are more evolved and produce more clusters than their Gaussian counterparts, while underdense regions are less evolved (*e.g.* grid lines are still visible). For negative $f_{\rm NL}$, underdense regions are more evolved, producing deeper voids, while overdense regions are less evolved, as illustrated by the grid lines apparent in the left of the top panel.

https://arxiv.org/pdf/0710.4560.pdf

Why higher multipole moments give longer runtimes

$$\mathrm{j}_n(z) = \frac{z^n}{2^{n+1} n!} \int_0^{\pi} \cos\,(z \cos\theta)(\sin\theta)^{2n+1}\,\mathrm{d}\theta.$$

Applications of our code

Theory				Data
$P(\vec{k})$	$\longrightarrow$ Convert to SFB	$C_\ell(k, k')$	$\longleftarrow$ Apply data	$n(\vec{r})$

Gauss-Legendre quadrature

$$\int_{-1}^{1} f(x)\,dx \approx \sum_{i=1}^{n} w_i\, f(x_i)$$

Density contrast

$$\delta = \frac{\rho - \bar{\rho}}{\bar{\rho}}$$